A Rapid Detection of Meat Spoilage using an Electronic Nose and Fuzzy-Wavelet systems

Kodogiannis, V.

This is an author's accepted manuscript of a conference paper published in Bi, Y., Kapoor, S., Bhatia, R. (eds) Proceedings of SAI Intelligent Systems Conference (IntelliSys) 2016. IntelliSys 2016. Lecture Notes in Networks and Systems, vol 15. Springer, Cham.

The final publication is available at Springer via:

https://dx.doi.org/10.1007/978-3-319-56994-9_36

A Rapid Detection of Meat Spoilage using an Electronic Nose and Fuzzy-Wavelet systems

Vassilis S. Kodogiannis
Faculty of Science and Technology
University of Westminster
London, United Kingdom
V.Kodogiannis@westminster.ac.uk

***Abstract*—Freshness and safety of muscle foods are generally considered as the most important parameters for the food industry. To address the rapid detection of meat spoilage microorganisms during aerobic or modified atmosphere storage, an electronic nose with the aid of fuzzy wavelet network has been considered in this research. The proposed model incorporates a clustering pre-processing stage for the definition of fuzzy rules. The dual purpose of the proposed modelling approach is not only to classify beef samples in the respective quality class (*i.e.* fresh, semi-fresh and spoiled), but also to predict their associated microbiological population directly from volatile compounds fingerprints. Comparison results against neural networks and neurofuzzy systems indicated that the proposed modelling scheme could be considered as a valuable detection methodology in food microbiology.**

Keywords—Fuzzy systems; neural networks; clustering; meat spoilage; modelling; classification; wavelets

I. INTRODUCTION

One of the most commonly consumed food item globally is meat, including beef. However, the shelf life of meat is low and the consumption of spoiled meat products could cause serious health hazards. Ensuring fast and reliable systems to determine safety/quality of meat products would benefit the public immensely, and also prevent unnecessary economic losses. Beef is one of the commercially extensively consumed muscle foods throughout the world. Although it is a good food source for proteins and other vital nutrients, it is also considered as an ideal substrate for the growth of pathogenic microorganisms and consequently spoilage.

Spoilage usually occurs when the formation of off-flavours, off-odours, discoloration, or any other changes in physical appearance or chemical characteristics make the food unacceptable to the consumer. Currently, meat safety is mainly relied on regulatory inspection and sampling protocols. This methodology, however, seems insufficient because it cannot guarantee consumer protection, as 100% inspection and sampling is simply difficult to be achieved. Additionally, although more than 50 chemical and microbiological methods have been proposed for the detection and measurement of bacterial spoilage in meat, most of them are considered as time-consuming processes [1]. Hence, the development of rapid and non-invasive sensors to detect spoilage and pathogenic bacteria is very desirable for Meat Industry. Various methods based on analytical instrumental techniques, such as Fourier transform infrared spectroscopy (FTIR) [2], Raman spectroscopy [3] and hyperspectral imaging [4] have been investigated for their potential in assessing meat quality. The "mechanism" of these approaches is based on the assumption that the metabolic activity of micro-organisms on meat results in biochemical changes, with the simultaneous formation of metabolic by-products, which could contribute to spoilage. The quantification of these metabolic activities is associated to a unique "signature", providing thus information about the type and rate of spoilage [5].

In the past two decades, awareness about the food safety from the point of specific pathogenic bacteria has considered the need for a rapid and accurate detection system for microbial spoilage by checking the volatile organic compounds (VOCs) generated by these microorganisms [6]. The practical application of human nose as a smell assessment instrument is limited by the fact that our sense of smell is subjective, gets tired easily, and is therefore difficult to use. Consequently, there was substantial need for an instrument that could mimic the human sense of smell and its use in routine industrial applications. To promote this technology to industrial application, gas/odour sensors became exemplary candidates in areas like food industry, environment control, automobile industry, indoor air quality check and monitoring, industrial production and medicine [7].

The electronic nose (enose) is a system initially created to mimic the function of human nose. An enose consists of an array of chemical gas sensors with broad and partly overlapping selectivity that measure volatile compounds, a signal-preparation system, and a pattern-recognition system. Such device is usually characterised by reproducibility and reliability. It is also highly efficient, with a short reaction and recovery time as well as a low cost. Although this instrument does not allow the identification of compounds and has a high detection limit in comparison with GC–MS, it has been successfully used in processing monitoring, shelf-life investigation, freshness evaluation and authenticity assessment in a wide range of food products, including meat products [8].

The main applications of enose with respect to meat are in assessing quality, spoilage identification, detection of off-flavours, taints and classification of bacterial strains. In one of the earliest research studies in the application of enose to meat

quality analysis, the changes in the headspace of vacuum packaged beef strip sides vaccinated with *Salmonella typhimurium* were evaluated using a metal oxide based enose [9]. The volatile compounds of pork, other meats and meat products such as sausages were also studied using an enose for halal verification [10]. An enose, consisting 18 MOS gas sensors, has been used for measuring and modelling flavour quality changes of refined chicken fat during controlled oxidation. Partial least squares regression (PLS) was utilised as a prediction model [11]. An integrated olfactory sensor system has been considered for the detection of Salmonella contamination in packaged beef steaks utilising neural network classifiers [12]. The prediction of total viable counts (TVC) in chilled pork using an enose using support vector machine (SVM) has been also investigated. In this specific experiment, enose and bacteriological measurements were performed on pork samples stored at 4 °C for up to 10 days [13].

The main objective of this paper is to associate, for the first time according to literature, volatile fingerprints (snapshots) of odour profile with beef spoilage through a multi-input-multi-output (MIMO) clustering-based fuzzy wavelet neural network (CFWNN) system. The proposed CFWNN system classifies beef fillets stored either aerobically or under modified atmosphere packaging to one of three quality classes (*i.e.* fresh, semi-fresh, and spoiled) and simultaneously predicts the microbial load (as total viable counts – TVC) on meat surface, based on the biochemical profile provided by the enose dataset. Results from CFWNN scheme are compared against models based on Adaptive Neural Fuzzy Inference System (ANFIS) and multilayer neural networks (MLP). Such comparison is considered as a essential test, as we have to emphasise the need of induction to the area of food microbiology, advanced learning-based modelling schemes, which may have a significant potential for the accurate estimation of meat spoilage.

II. Experimental Case

A. Sample Preparation and Microbiological Analysis

The entire experimental case study was performed at the Agricultural University of Athens, Greece. A detailed description of the experimental methodology, as well as the related microbiological analysis of the meat samples, is described in [14]. Briefly, the samples were prepared by cutting fresh pieces of beef into small pieces and then stored aerobically (AIR) and in modified atmosphere packaging (MAP) (40% CO_2, 30% O_2, 30% N_2) at different temperatures. Meat samples were stored under controlled isothermal conditions at 0, 4, 8, 12, 16 and 20°C in high precision incubators for up to 434 h, depending on storage temperature, until spoilage was pronounced. At the beginning and during storage, after appropriate time intervals, duplicate meat samples were taken for microbiological, sensory and chemical analysis via enose. It was assumed that the microbial population at these parts would be comparable. Samples were not subjected to any prior pre-treatment such as fat and connective tissue removal, or inoculation with selected species of bacteria. Samples stored under aerobic conditions were analyzed every 24, 24, 12 and 8 h for 0, 4, 8 and 12°C respectively. Finally, samples stored at 16 and 20°C were analyzed at 4–6 h intervals. Similarly, samples stored under MAP conditions were analyzed every 48, 24, 16, 12, 8 and 6 h for 0, 4, 8, 12, 16 and 20°C respectively.

In parallel, microbiological analysis was performed, and resulting growth data from agar plate counts were $\log_{10}$ transformed and fitted to the primary model of Baranyi in order to verify the kinetic parameters of microbial growth (maximum specific growth rate and lag phase duration) [14].

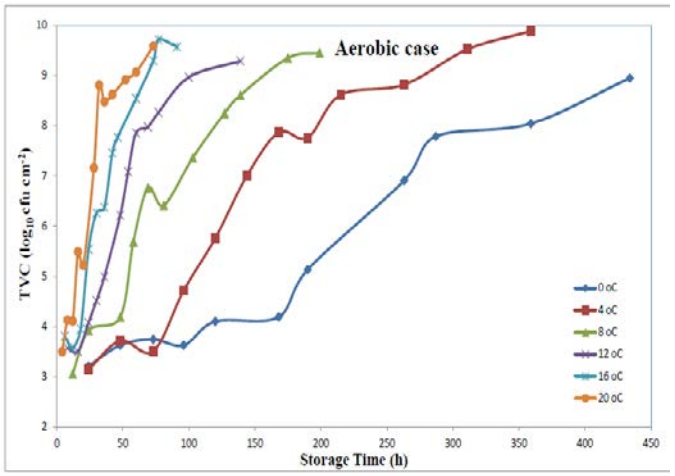

Fig. 1. Population dynamics of TVC at various temperatures (AIR)

The growth curves of total viable counts (TVC) for beef fillet storage at different temperatures under aerobic and MAP conditions as a function of storage time are illustrated in Figs 1&2. The growth curves for both TVC cases are similar, with the exception that the maximum specific growth rate (μmax) for the AIR packaged condition is different than of that of the MAP case.

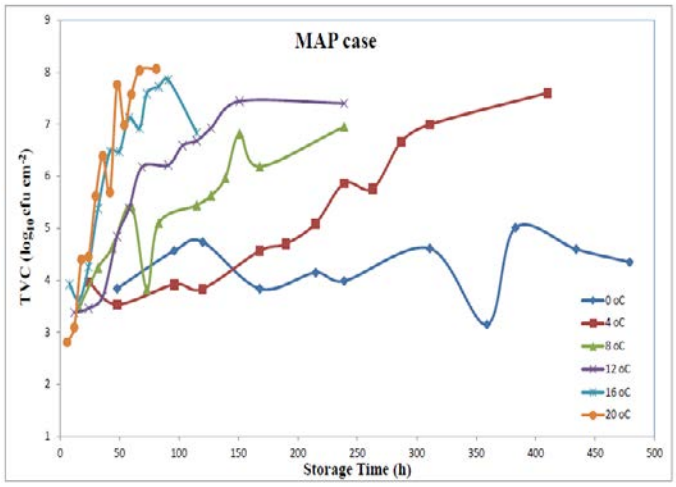

Fig. 2. Population dynamics of TVC at various temperatures (MAP)

It has been found that packaging under modified atmosphere delay the growth rates of all members of the microbial association, as well as the maximum population attained by each microbial group compared with aerobic storage. Aerobic storage accelerates spoilage due to the fast growing

Pseudomonas spp.; in addition such growth can be significantly inhibited by the presence of gas carbon dioxide [15]. However, for both aerobic and MAP conditions, the growth rate is increased faster, as the storage temperature increases.

Additionally, sensory evaluation of meat samples was performed during storage, based on the perception of colour and smell before and after cooking [14]. Each sensory attribute was assigned to a three-point scale corresponding to: 1=fresh (acceptable meat quality and the absence of off-flavours); 2=semi-fresh (presence of slight off-flavours but not spoiled); and 3= spoiled (clearly off-flavour development). In total, 210 meat samples were evaluated by a sensory panel and classified into the selected three groups as fresh (n = 48), semi-fresh (n = 72), and spoiled (n = 90) for the aerobic case, while 213 meat samples were classified as fresh (n = 51), semi-fresh (n = 84), and spoiled (n = 78) for the MAP case.

B. Volatile Samples Acquisition

Libra enose is a compact analytical device used to identify complex odours produced by Technobiochip [16]. The instrument is composed by an array of sensors and a data analysis system. Sensors work like biological receptors and the data analysis system allows transposing extracted from an odour in an "olfactory" image analogous with our "sensation" of a smell. The detection of odours is then likely as different odours have different "olfactory" images. This distinguishes enose from gas chromatography which identifies and measure single molecular classes inside a gaseous mixture. Enose recognises an odour as a whole, showing the synergic activity of different molecular species in a single "olfactory" image.

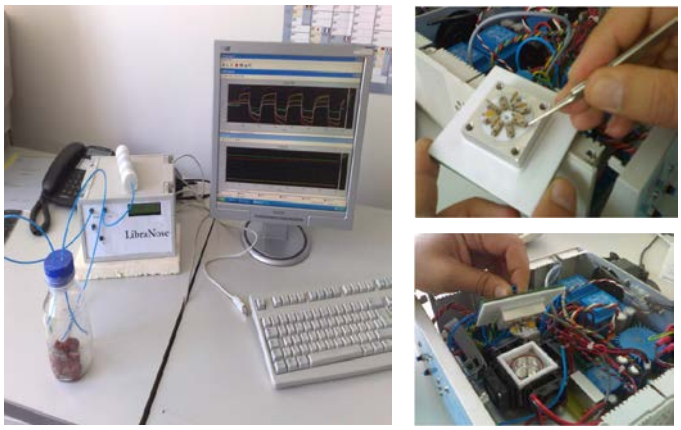

Fig. 3. Libra Electronic Nose

Libra enose uses a set of eight 20MHz piezoelectric transducers placed in a measuring chamber. Fig 3 illustrates its details. The device can be quickly reused after a short cycle of cleaning using clean filtered air obtained via a carbon active filter. The measuring chamber is held at a constant temperature during the measurements by a thermostatic electronic system. A flow system formed by a micro-electric valve and a micro-pump conveys the gas sample to the measuring chamber in a controlled, by the connected computer, way. For each measurement, a beef fillet sample of 5 g was introduced inside a 100 ml volume glass jar and left at room temperature (20°C ±2°C) for 15 min to enhance desorption of volatile compounds from the meat into the headspace. The headspace was then pumped over the sensors of the electronic nose and the generated signal was continuously recorded to a computer.

Datasets related to volatile extracted information from Libra enose as well as the associated microbiological analysis from meat samples for both aerobic and MAP cases, were provided by Agricultural University of Athens, Greece and were further utilised towards the development of the proposed intelligent model.

III. CFWNN ARCHITECTURE

Generally, the FWNN is a combined structure based on fuzzy rules that includes wavelet functions in their consequent parts, in the form of a wavelet neural network. In these FWNN schemes, such combination is achieved through a Takagi–Sugeno–Kang (TSK) structure, which allows us to develop a system that has fast training speed, and describe nonlinear objects that are characterized with uncertainty. The domain interval of each input is separated into fuzzy regions and each region is associated with a membership function (MF) in the IF part of the fuzzy rules. The rules are then defined either by experts or are learnt adaptively similarly to ANFIS scheme [17].

In this research study, a novel Multi-Input Multi-Output (MIMO) Clustering Fuzzy Wavelet Neural Network (CFWNN) is proposed for the detection of meat spoilage. In the general case of FWNNs, the number of fuzzy rules is important as it affects the accuracy and the efficiency of the developed prediction system. A second problem is related to the initialization stage. In fact the initial parameters of the network greatly affect the accuracy result, the time required for learning and even the convergence and stability of the training process.

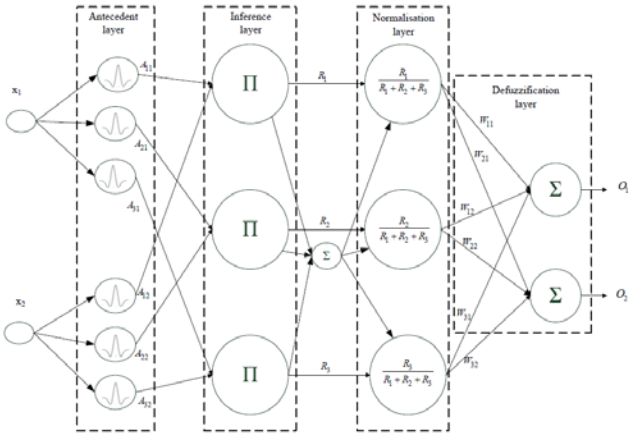

Fig. 4. CFWNN architecture

A clustering algorithm is applied initially, as a pre-processing step, to the training dataset in order to organize feature vectors into clusters, such that points within a cluster are closer to each other than vectors belonging to different clusters. The fuzzy rule base is derived using results obtained from a clustering algorithm. In the proposed scheme, the number of memberships for each input variable is directly associated to

the number of rules, hence, the "*curse of dimensionality*" problem is significantly reduced. Fig. 4 illustrates the architecture of the MIMO CFWNN architecture.

Gaussian membership functions (MF) are commonly used in Neuro-Fuzzy (NF) systems. A deficiency of Gaussian-based NF networks is their limited ability to localize in the frequency domain. By comparison, the proposed CFWNN, where wavelet functions are utilized, has the ability to localize in both the time and frequency domains. In this paper, the following generalized Mexican Hat wavelet function with translation (μ) and dilation (σ) parameters has been considered as MF:

$$\psi\left(\frac{x-\mu}{\sigma}\right)=\left(1-\left(\frac{x-\mu}{\sigma}\right)^2\right)\exp\left(-0.5\left(\frac{x-\mu}{\sigma}\right)^2\right) \quad (1)$$

Translation parameter determines the center position of the wavelet, while dilation parameter controls the spread of the wavelet. As MF values cannot be negative and larger than unity, the Mexican Hat MF has been normalized as follows:

$$A_{ij}=\frac{\left(1-\left(\frac{x_i-\mu_{ij}}{\sigma_{ij}}\right)^2\right)\exp\left(-0.5\left(\frac{x_i-\mu_{ij}}{\sigma_{ij}}\right)^2\right)+\varepsilon}{1+\varepsilon} \quad (2)$$

where constant $\varepsilon=0.446$. The structure of the CFWNN is explained below layer by layer:

- **Layer 1:** This layer is simply the input layer. Nodes in this layer pass on the input signals $x_1, x_2, ..., x_n$ to L_2.
- **Layer 2:** This layer is the fuzzification layer, and its nodes represent the fuzzy sets used in the antecedent parts of the fuzzy rules. A fuzzification node receives an input and determines the degree to which this input belongs to in the node's fuzzy set. The outputs of this layer are the values of wavelet MFs for the input values. The normalised Mexican Hat MF A_{ij} presented at Eq. 2 have been utilized for the proposed CFWNN, where, index j is associated with the input variable, while index i is linked with MF's j^{th} input. The initial translation variables μ_{ij} at Eq. 3 are equal to the values of the components of the vectors $\boldsymbol{v_i}$, which come from the second stage of the clustering pre-processing step. The dilation values σ_{ij} are initialised according to

$$\sigma_{ij}=\left(\sum_{k=1}^{n}u_{ik}(x_{kj}-v_{ij})^2\Big/\sum_{k=1}^{n}u_{ik}\right)^{1/2} \quad (3)$$

  These values are calculated based on the matrix $\mathbf{U}$, where its elements correspond to the fuzzy memberships of $\boldsymbol{x_k}$ in the i^{th} cluster and have values obtained again from the fuzzy c-means part of the clustering step.
- **Layer 3:** This layer is the firing strength calculation layer. Since each fuzzy rule's antecedent part has AND connection operator, the firing strengths are calculated using the product T-norm operator. The most commonly used fuzzy AND operations are intersection and algebraic product. In this case, the multiplication has been used, and the output of this layer has the following form:

$$R_j=\prod_{i}^{n}A_{ji}(x_i) \quad (4)$$

  The number of nodes, at this layer, is equal to the number of clusters, as it was defined by the clustering pre-processing step.
- **Layer 4**: This layer is the normalization layer. Each node in this layer calculates the normalized activation strength of each rule by:

$$\overline{R}_i=\frac{R_i}{\sum_{j=1}^{c}R_j} \quad (5)$$

  The normalized activation strength is the ratio of the activation strength of a given combination to the sum of activation strengths of all combinations. It represents the contribution of a given combination to the final result.
- **Layer 5**: This layer is related to the defuzzification /output part of the CFWNN. Each node at this layer combines the output of each node in L_4 by algebraic sum operation after being multiplied by the output weight value w_{ij}:

$$O_i=\sum_{j=1}^{c}w_{ij}\overline{R}_j \quad (6)$$

A. Clustering-based Initialization

The applied clustering algorithm at layer L2 consists of two stages [18]. In the first stage the method similar to Learning Vector Quantization (LVQ) algorithm generates crisp c-partitions of the data set. The number of clusters c and the cluster centres v_i, $i=1,...,c$, obtained from this stage are used by Fuzzy c-means (FCM) algorithm in the second stage. The first stage clustering algorithm determines the number of clusters by dividing the learning data into these crisp clusters and calculates the cluster centres which are the initial values of the fuzzy cluster centres derived the second stage algorithm. Let $\boldsymbol{X}=[\boldsymbol{x}_1,...,\boldsymbol{x}_n] \in \mathrm{R}^{np}$ be a learning data. The first cluster is created starting with the first data vector from X and the initial value of the cluster centre is taking as a value of this data vector. Then other data vectors are included into the cluster but only these ones which satisfy the following condition

$$\|x_k-v_i\|<D \quad (7)$$

where $x_k \in X, k=1,...,n$ and $v_i, i=1,...,c$ are cluster centres, $V=[v_1,...,v_n] \in \mathrm{R}^{cp}$, the constant value D is fixed at the beginning of the algorithm. Cluster centres v_i are modified for each cluster (i.e., $i=1,...,c$) according to the following equation

$$v_i(t+1) = v_i(t) + a_t(x_k - v_i(t)) \quad (8)$$

where $t = 0,1,2,..$ denotes the number of iterations, $a_t \in [0,1]$ is the learning rate and it is decreasing during the execution of the algorithm (depending on the number of elements in the cluster). At the end of first stage, the number of clusters c is defined, while the dataset is divided into the clusters. In addition, the values of cluster centres v_i, $i = 1,...,c$, which can be used as initial values for the second stage clustering algorithm, are calculated. In the second stage the fuzzy c-means algorithm has been used to optimize the values of cluster centres.

B. CFWNN Learning Phase

The learning algorithm of CFWNN involves the use of the gradient descent (GD) method to optimize the various network parameters. For each training pair (x, y), the system output O_i is obtained in forward pass after feeding an input pattern into the network. Then the purpose of this learning phase is that, for a given p^{th} training data pair (x_p, y_p), the parameters are adjusted so as to minimize the error function

$$E = \frac{1}{2}\sum_{p=1}^{P}(D_p - O_p)^2 \quad (9)$$

where P is the number of outputs and D_p the desired response of the p^{th} output. Variable O_p is defined as in Eq. 6. According to the GD method, the weights in the defuzzification layer are updated by the following equation

$$\Delta W_{ij} = -\frac{\partial E}{\partial W_{ij}} = -\frac{\partial E}{\partial O_i}\frac{\partial O_i}{\partial W_{ij}} = (D_i - O_i)\bar{R}_j \quad (10)$$

where $i = 1,2,..,p$ and $j = 1,2,..c$ denote the number of output and normalization units respectively. The weights of the output units are updated according to the following equation

$$W_{ij}(t+1) = W_{ij}(t) + \eta \Delta W_{ij} \quad (11)$$

where η is the learning rate. The μ_{ij} and σ_{ij} parameters of the wavelet membership function are adjusted by the amount

$$\begin{aligned} \mu_{ij}(t+1) &= \mu_{ij}(t) - \eta_\mu \left(\frac{\partial E}{\partial \mu_{ij}}\right). \\ \sigma_{ij}(t+1) &= \sigma_{ij}(t) - \eta_\sigma \left(\frac{\partial E}{\partial \sigma_{ij}}\right) \end{aligned} \quad (12)$$

$\frac{\partial E}{\partial \mu_{ij}}$, $\frac{\partial E}{\partial \sigma_{ij}}$ components need to be calculated using the chain rule

$$\frac{\partial E}{\partial \mu_{ij}} = \frac{\partial E}{\partial \bar{R}_j}\frac{\partial \bar{R}_j}{\partial R_j}\frac{\partial R_j}{\partial A_{ij}}\frac{\partial A_{ij}}{\partial \mu_{ij}} \quad (13)$$

and

$$\frac{\partial E}{\partial \sigma_{ij}} = \frac{\partial E}{\partial \bar{R}_j}\frac{\partial \bar{R}_j}{\partial R_j}\frac{\partial R_j}{\partial A_{ij}}\frac{\partial A_{ij}}{\partial \sigma_{ij}} \quad (14)$$

Analytically, the partial derivatives are defined as

$$\frac{\partial E}{\partial \bar{R}_j} = -\sum_{i=1}^{p}(D_i - O_i)w_{ij} \quad (15)$$

$$\frac{\partial \bar{R}_j}{\partial R_j} = \frac{\sum_{i=1}^{c} R_i - R_j}{\left(\sum_{i=1}^{c} R_i\right)^2} \quad (16)$$

$$\frac{\partial R_j}{\partial A_{ij}} = \prod_{i \neq j} A_{ij} \quad (17)$$

$$\begin{aligned} &\frac{\partial A_{ij}}{\partial \mu_{ij}} = \frac{1}{1+\varepsilon}A, \\ &A = \left(\frac{(x_j - \mu_{ij})}{(\sigma_{ij})^2}\left(3 - \frac{(x-\mu)^2}{(\sigma_{ij})^2}\right)\exp\left(-\frac{1}{2}\left(\frac{(x-\mu)^2}{(\sigma_{ij})^2}\right)\right)\right) \end{aligned} \quad (18)$$

and

$$\begin{aligned} &\frac{\partial A_{ij}}{\partial \sigma_{ij}} = \frac{1}{1+\varepsilon}B \\ &B = \left(\frac{(x_j - \mu_{ij})^2}{(\sigma_{ij})^3}\left(3 - \frac{(x-\mu)^2}{(\sigma_{ij})^2}\right)\exp\left(-\frac{1}{2}\left(\frac{(x-\mu)^2}{(\sigma_{ij})^2}\right)\right)\right) \end{aligned} \quad (19)$$

All modelling schemes have been implemented in MATLAB (ver. R2014a, Mathworks.com).

IV. Decision Support System Development

A machine learning approach, based on the proposed CFWNN model, has been adopted in order to create a decision support system acting in parallel as an efficient classifier, in an effort to classify meat samples in three quality classes (fresh, semi-fresh, spoiled), as well as a prediction system. The real challenge in this paper is to propose a learning-based structure which could be considered as a new benchmark method towards the development of efficient intelligent methods in food quality analysis. For this reason, CFWNN's results are compared with those obtained by MLP neural networks, and ANFIS neurofuzzy identification models which are considered as well-recognised tools in chemometric analysis. The proposed concept involves the development of two CFWNN models for aerobic and MAP storage respectively.

Pre-processing of the data obtained from enose sensors is required to obtain the "olfactory image" of the sample. This process involves extracting certain significant characteristics from the sensor response curves in order to produce a set of data that can be processed by the recognition system of the enose. Different features can be extracted and used depending

on the characteristics of the enose used such as the type of sensors adopted, and the stability of the responses of the latter to the reference gas, to variations in humidity and temperature levels.

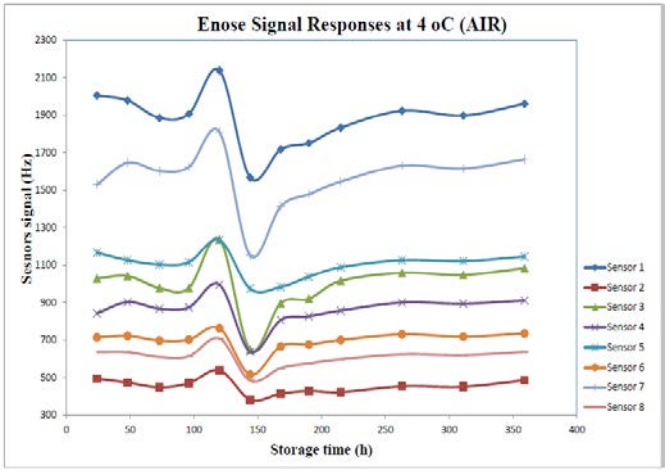

Fig. 5. Enose responses during storage of beef fillets at 4°C (AIR)

The responses of all sensor signals classes for meat samples stored at 4°C are for the aerobic case are shown in Fig. 5, while the related diagram for the MAP case in Fig. 6.

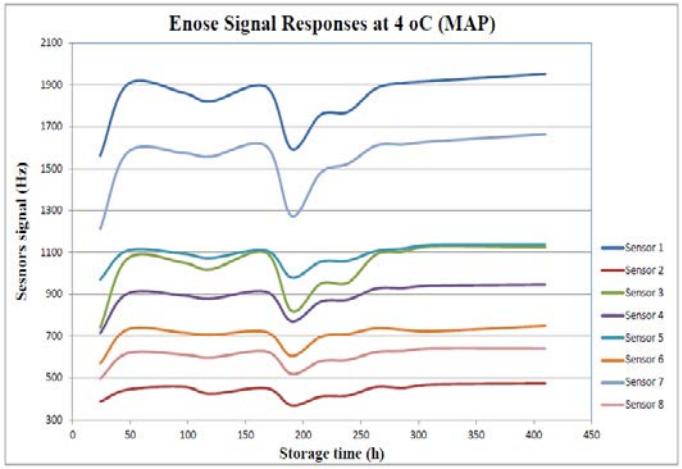

Fig. 6. Enose responses during storage of beef fillets at 4°C (MAP)

Considering that each measurement can be represented as a point in an 8-dimensional space, a dimensionality reduction algorithm has been applied on those enose data used for training purposes. The robust PCA (RPCA) scheme has been utilized to obtain principal components that are not influenced much by outliers. The RPCA procedure is implemented in three main steps. First, the data were pre-processed such that the transformed data are lying in a subspace whose dimension is at most $n-1$. A preliminary covariance matrix was then constructed and used for selecting the number of components k that will be retained in the sequel, yielding a k-dimensional subspace that fits the data well. Then the data points were projected on this subspace where their location and scatter matrix are robustly estimated, from which its k nonzero eigenvalues $l_1,...,l_k$ are computed. The corresponding eigenvectors are the k robust principal components [19]. RPCA scheme was implemented in MATLAB, with the aid of PLS_Toolbox (ver. 8.0 Eigenvector.com).

TABLE I. ROBUST PCA SCHEME

PCs	Robust PCA		
	Eigenvalue	Prop. %	Cum. prop. %
1	7.17e+004	71.45	71.45
2	1.11e+004	21.88	93.34
3	2.40e+003	4.11	97.45
4	9.47e+002	1.55	99.01
5	2.70e+002	0.50	99.50

For this particular experimental case study, the first four principal components (PC) were associated with the 99% of the total variance, as shown in Table I. These specific PCs were extracted and utilised as inputs variables to the learning-based models developed for this specific case study, together with information from the various storage temperatures, as well as the related sampling times. A mandatory check however is required to validate the integrity and applicability of the developed models in predicting/classifying unknown samples to make sure that models could work in the future for new and similar data. For the aerobic and MAP cases, 140 and 142 samples were considered as training subsets respectively, while remaining 70 and 71 samples were included in the testing subsets.

V. RESULTS & DISCUSSION

A. Aerobic storage case study

CFWNN's structure consists of an input layer which contains six input nodes (i.e. storage temperature, sampling time, and the values of the first four principal components). The output layer consists of two nodes, corresponding to the predicted quality class (fresh, semi-fresh, spoiled) of meat samples and the related microbiological attribute, respectively. As both output parameters are not independent, in the sense that quality class is related to microbiological counts and vice versa, a model that combines both these measurements have been considered to be desirable.

In the proposed CFWNN model, 10 final rules have been created, using the clustering pre-processing stage. Although the classic GD method utilised as a learning scheme, the training time was completed in less than 1000 epochs, much faster from the equivalent time used to train the MLP neural network. The classification accuracy of the model was determined by the number of correctly classified samples in each sensory class divided by the total number of samples in the class. The performance of the model for the prediction of TVC for each meat sample was determined by the bias (B_f) and accuracy (A_f) factors, the mean relative percentage residual (MRPE) and the mean absolute percentage residual (MAPR), and finally by the root mean squared error (RMSE) and the standard error of prediction (SEP) [20].

Results revealed that the classification accuracy of the CFWNN model was very satisfactory in the characterization of beef samples, indicating the advantage of a hybrid intelligent

approach in tackling complex, nonlinear problems, such as meat spoilage. The classification accuracy is presented in the form of a confusion matrix in Table II. The model overall achieved a 95.7% correct classification, and 100%, 87.5% and 100% for fresh, semi-fresh and spoiled meat samples, respectively.

TABLE II. CONFUSION MATRIX FOR CFWNN (AIR)

True class	Predicted class (AIR)			Row total (n_i)	Sensitivity (%)
	Fresh	Semi-fresh	Spoiled		
Fresh (n = 16)	15+1(marginal)	0	0	16	100
Semi-fresh (n = 24)	2	20+1(marginal)	1	24	87.5
Spoiled (n = 30)	0	0	29+1(marginal)	30	100
Column total (n_j)	18	21	31	70	
Specificity (%)	88.88	100	96.77		
Overall correct classification (accuracy): 95.71%					

The sensitivity (*i.e.* how good the network is at identifying correctly the positive samples) as well as the specificity index (*i.e.* how good the network is at identifying correctly the negative samples) were high, indicating satisfactory discrimination between these three classes. It is characteristic that no fresh samples were misclassified as spoiled and vice versa, indicating that the biochemical information provided by enose data could discriminate these two classes accurately.

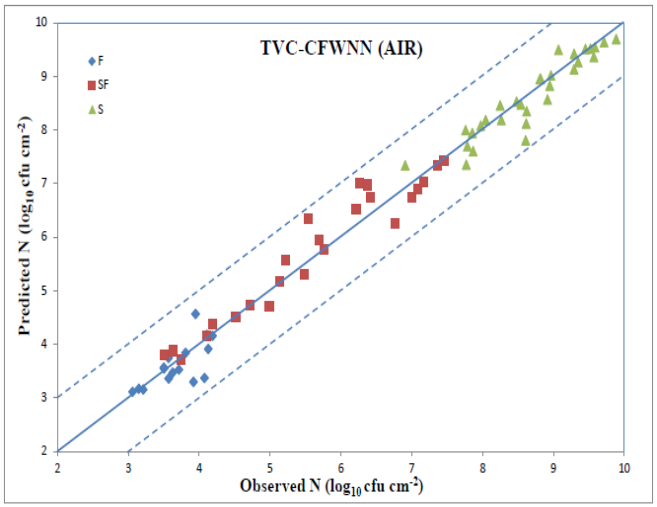

Fig. 7. CWFNN prediction model for TVC (AIR)

The plot of predicted (via CFWNN) versus observed total viable counts is illustrated in Fig. 7, and shows a very good distribution around the line of equity (y=x), with all the data included within the ±1 log unit area. A more comprehensible picture of the CFWNN's prediction performance is however provided in Fig 8 where the % relative error of prediction is shown against the observed microbial population. Based on this plot, data were distributed above and below 0, with approximately the majority of predicted microbial counts included within the ± 10% RE zone. Samples "6A9", "8A9", "10A9", "8A5", and "8A7" are clearly placed outside the ± 10% RE zone. The "6A9", "8A9", "10A9", cases correspond to AIR samples stored at the same time (16 ^{o}C) and collected at 18h, 24h and 30h respectively. The cases "8A5" and "8A7" correspond to AIR samples collected at 24h and stored at 10 ^{o}C and 12 ^{o}C respectively.

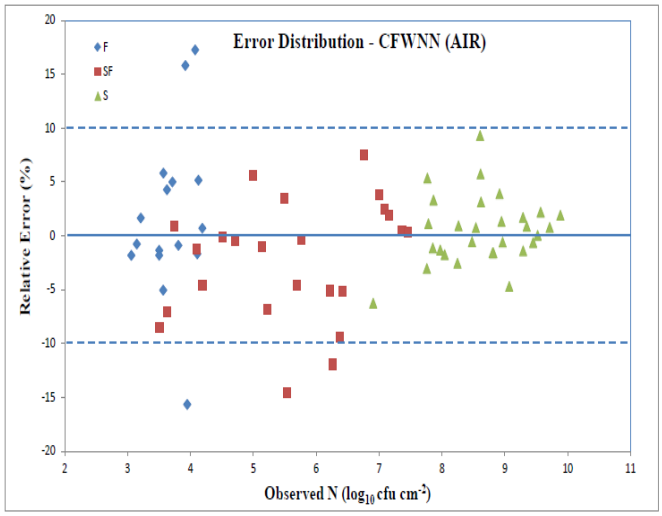

Fig. 8. CFWNN's Residual Error performance (AIR)

The performance of the CFWNN model to predict TVCs in beef samples in terms of statistical indices is presented in Table III. Based on the calculated values of the bias factor B_f, it can be assumed that the proposed model under-estimated TVCs in fresh and spoiled samples (B_f <1), whereas for semi-fresh samples over-estimation of microbial population was evident (B_f >1). The overall B_f was almost optimal (ca. 1.0).

TABLE III. PERFORMANCE OF CFWNN MODEL FOR TVC

Statistical index (AIR) - CWNN	Fresh	Semi-fresh	Spoiled	Overall
Mean squared error (MSE)	0.0911	0.1112	0.0681	0.0881
Root mean squared error (RMSE)	0.3019	0.3334	0.2610	0.2969
Mean relative percentage residual (MRPR %)	1.6654	-2.2672	0.5252	-0.1716
Mean absolute percentage residual (MAPR %)	5.2899	4.4713	2.3303	3.7409
Bias factor (B_f)	0.9805	1.0212	0.9943	1.0002
Accuracy factor (A_f)	1.0559	1.0446	1.0238	1.0382
Standard error of prediction (SEP %)	8.1776	5.9582	3.0053	4.5785

The mean relative percentage residual index (MRPR) similarly verified the over-prediction for semi-fresh samples (MRPR < 0) and under-prediction for fresh and spoiled samples (MRPR > 0). Finally, the standard error of prediction (SEP) index is a relative typical deviation of the mean prediction values and expresses the expected average error associated with future predictions. The value of the index was 4.57% for the overall samples, indicating good performance of the network for microbial count predictions. However in the case of fresh samples, the index gave higher values (i.e. 8.17%).

In addition to CFWNN, in this research work, an ANFIS and an MLP neural model have been developed to predict TVCs. The same validation technique, as well as the same training dataset has been utilized also for these cases. Under these conditions, ANFIS performed satisfactory, its performance however was achieved with a high computational cost, by utilizing two membership functions for each input variables and 64 fuzzy rules. Statistical information for ANFIS model is illustrated at Table IV. MLP was implemented with two hidden layers (with 12 and 6 nodes respectively) and two output nodes, one for the sensory class and one for the TVCs.

TABLE IV. PERFORMANCE OF ANFIS MODEL FOR TVC

Statistical index (ANFIS case) - AIR	Fresh	Semi-fresh	Spoiled	Overall ANFIS	Overall MLP
Mean squared error (MSE)	0.1858	0.2943	0.1821	0.2214	0.2397
Root mean squared error (RMSE)	0.4310	0.5425	0.4267	0.4705	0.4896
Mean relative percentage residual (MRPR %)	-2.3051	0.0791	0.7813	-1.1780	-0.4163
Mean absolute percentage residual (MAPR %)	8.7771	7.9101	3.6923	6.3007	6.2523
Bias factor (B_f)	1.0162	1.0245	0.9909	1.0081	1.0002
Accuracy factor (A_f)	1.0924	1.0793	1.0381	1.0644	1.0643
Standard error of prediction (SEP %)	11.6759	9.6944	4.9139	7.2567	7.5514

B. *Modified Atmosphere Packaging case study*

An important advancement in food packaging techniques is the development of Modified Atmosphere Packaging (MAP). Modified atmospheric packaged foods have become increasingly more available, as food manufactures are interested for foods with extended shelf life. In addition to aerobic TVCs prediction, a CFWNN model has been also applied for meat samples packaged under modified atmosphere conditions. For this particular case, 14 final rules have been created, using the clustering pre-processing stage.

TABLE V. CONFUSION MATRIX FOR CFWNN (MAP)

True class	Predicted class (MAP)			Row total (n_i)	Sensitivity (%)
	Fresh	Semi-fresh	Spoiled		
Fresh (n = 17)	15+1(marginal)	1	0	17	94.11
Semi-fresh (n = 28)	1	23+2(marginal)	2	28	89.28
Spoiled (n = 26)	0	1	24+1(marginal)	26	96.15
Column total (n_j)	17	27	27	71	
Specificity (%)	94.11	92.59	92.59		
Overall correct classification (accuracy): 92.95%					

The classification accuracy of CFWNN model again it was very satisfactory in the characterization of beef samples, however, a comparison against CFWNN's performance for AIR case, reveals an increased level of difficulty in predicting/classifying meat samples packaged under MAP conditions. The classification accuracy is presented in the form of a confusion matrix in Table V. The model overall achieved a 92.95% correct classification, with 5 misclassifications, especially in the semi-fresh category. The sensitivity as well as the specificity index was obviously lower than the previous case.

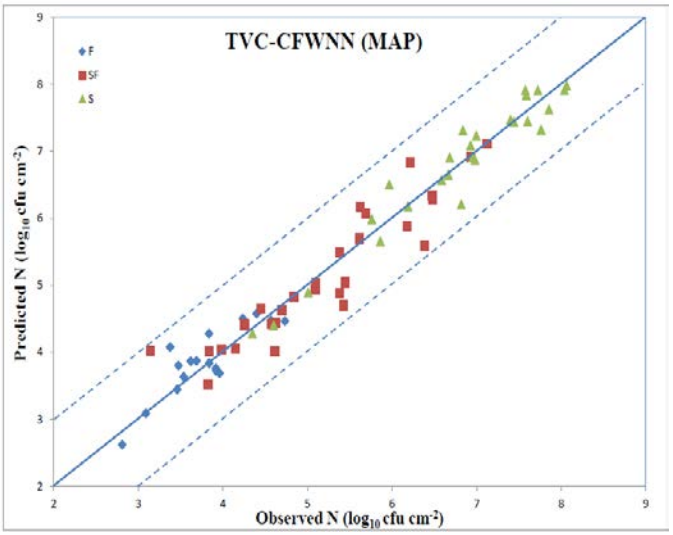

Fig. 9. CWFNN prediction model for TVC (MAP)

The plot of predicted vs. observed TVCs for MAP spectra is illustrated in Fig 9, and shows a good distribution around the line of equity, with all the data included within the ±1.0 log unit area. Based on Fig. 9, three samples (i.e. "12M11", "54M1", "22M5") were however in the border line of the ±1.0 log unit area. "12M11" corresponds to a beef sample stored at 20°C and collected after 36h of storage, while "54M1" corresponds to a sample stored at 0°C and collected after 359h of storage. Finally, "22M5" corresponds to a beef sample stored at 8°C and collected after 60h of storage.

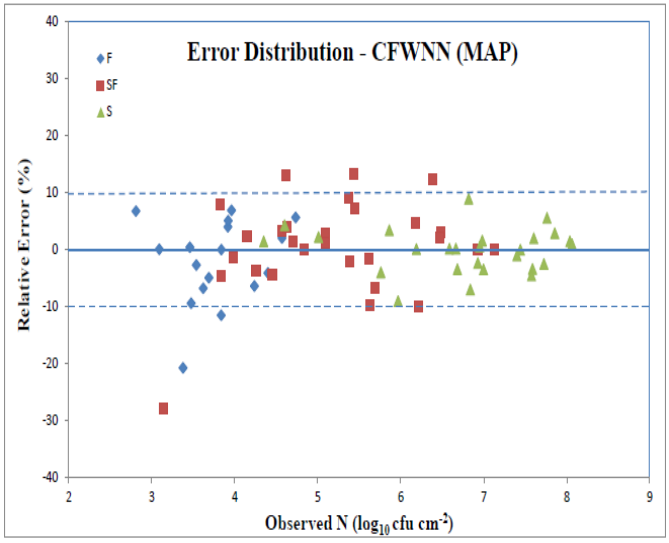

Fig. 10. CFWNN's Residual Error performance (MAP)

Similarly to the aerobic case, CFWNN's prediction performance is also illustrated in Fig 10 where the % relative error of prediction is shown against the observed microbial population. Based on this plot, data were distributed above and

below 0, with approximately the majority of predicted microbial counts included within the ± 10% RE zone.

TABLE VI. PERFORMANCE OF CFWNN MODEL FOR TVC

Statistical index (CFWNN case) MAP	Fresh	Semi-fresh	Spoiled	Overall
Mean squared error (MSE)	0.0737	0.1419	0.0652	0.0975
Root mean squared error (RMSE)	0.2715	0.3767	0.2554	0.3123
Mean relative percentage residual (MRPR %)	-2.066	0.6115	-0.1570	-0.3112
Mean absolute percentage residual (MAPR %)	5.7326	5.7387	2.9474	4.7151
Bias factor (B_f)	1.0182	0.9907	1.0008	1.0010
Accuracy factor (A_f)	1.0573	1.0589	1.0299	1.0478
Standard error of prediction (SEP %)	7.1594	7.2481	3.7681	5.7401

The performance of the CFWNN model to predict TVCs in beef samples in terms of statistical indices for this case is presented in Table VI. The mean relative percentage residual index (MRPR) revealed an under-prediction for semi-fresh samples (MRPR > 0) and over-prediction for fresh and spoiled samples (MRPR <0). Finally, the standard error of prediction (SEP) index was 5.74% for the overall samples, indicating an inferior performance compared to previous aerobic case. In addition to CFWNN, an ANFIS and an MLP neural model have been developed to predict TVCs for the MAP case. ANFIS performed less satisfactory, while MLP's performance revealed MLP's deficiency in handling highly non-linear problems. Table VII summarized these performances.

TABLE VII. PERFORMANCE OF ANFIS MODEL FOR TVC

Statistical index (ANFIS case) - MAP	Fresh	Semi-fresh	Spoiled	Overall ANFIS	Overall MLP
Mean squared error (MSE)	0.0870	0.2518	0.3238	0.2387	0.3029
Root mean squared error (RMSE)	0.2949	0.5018	0.5690	0.4886	0.5503
Mean relative percentage residual (MRPR %)	2.1699	-1.3843	1.2657	0.4371	1.2118
Mean absolute percentage residual (MAPR %)	5.9772	7.9051	6.0712	6.7719	7.8681
Bias factor (B_f)	0.9756	1.0079	0.9836	0.9912	0.9829
Accuracy factor (A_f)	1.0634	1.0799	1.0640	1.0701	1.0831
Standard error of prediction (SEP %)	7.7764	9.6556	8.3949	8.9815	10.1169

VI. CONCLUSIONS

In conclusion, this simulation study demonstrated the effectiveness of the detection approach based on electronic nose which in combination with an appropriate machine learning strategy could become an effective tool for monitoring meat spoilage during aerobic storage at various temperatures. The collected "volatile" data could be considered as biochemical "signature" containing information for the discrimination of meat samples in quality classes corresponding to different spoilage levels, whereas in the same time could be used to predict satisfactorily the microbial load directly from the sample surface. The realization of this strategy has been fulfilled with the development of a MIMO fuzzy-wavelet network which incorporates a clustering pre-processing stage. Classification performance was very satisfactory, while overall prediction for TVCs has been considered as very promising, although lower performance was observed especially for samples stored under MAP conditions. Prediction performances of MLP and PLS schemes revealed the deficiencies of these systems which have been used extensively in the area of Food Microbiology. There is need to explore further the use of hybrid intelligent systems, and this paper has attempted for the first time to associate enose data with such systems. Further research will be focused in incorporating to the data analysis, specific microbiological data, such as *Pseudomonas spp., Brochothrix thermosphacta,* Lactic acid bacteria and *Enterobacteriaceae.*

ACKNOWLEDGMENT

The author would like to thank Dr E.Z. Panagou from Agricultural University of Athens, Greece for providing the enose dataset, as well as the related microbiological analysis that correspond to beef samples.

REFERENCES

[1] Ellis D.I., Goodacre R., "Rapid and quantitative detection of the microbial spoilage of muscle foods: current status and future trends", Trends in Food Science & Technology, Vol. 12, pp. 414-424, 2001.

[2] Mouwen D.J.M., Hörman A., Korkeala H., Alvarez-Ordóñez A. Prieto, M., "Applying Fourier-transform infrared spectroscopy and chemo-metrics to the characterization and identification of lactic acid bacteria", Vibrational Spectroscopy, vol. 56, No. 2, pp. 193-201, 2011

[3] Wang, Q., Lonergan, S.M., Yu, C., "Rapid determination of pork sensory quality using Raman spectroscopy", Meat Science, vol. 91, No. 3, pp. 232-239, 2012

[4] Feng Y.Z., Sun D.W., "Application of hyperspectral imaging in food safety inspection and control: A review", Critical Reviews in Food Science and Nutrition, Vol. 52, pp. 1039–1058, 2012.

[5] Nicolaou, N., Goodacre, R., "Rapid and quantitative detection of the microbial spoilage in milk using Fourier transform infrared spectroscopy and chemometrics", Analyst, Vol. 133, No. 10, pp. 1424-1431, 2008.

[6] Boothe, D.D.H., Arnold, J.W., "Electronic nose analysis of volatile compounds from poultry meat samples, fresh and after refrigerated storage", Journal of the Science of Food and Agriculture, Vol. 82, No. 3, pp. 315-322, 2002.

[7] Capelli, L., Sironi, S., Del Rosso, R., "Electronic noses for environmental monitoring applications", Sensors, Vol. 14, No. 11, pp. 19979-20007, 2014.

[8] Di Natale C., Macagnano A. and D'Amico A., "Electronic nose and sensorial analysis: Comparison of performances in selected cases", Sensors & Actuators B, Vol. 50, pp. 246–252, 1998

[9] Balasubramanian, S., Panigrahi, S., Logue, C. M., Gu, H., & Marchello, M., "Neural networks integrated metal oxide based artificial olfactory system for meat spoilage identification", Journal of Food Engineering, Vol. 91, pp. 91–98, 2009.

[10] Nurjuliana, M., Che Man, Y.B., Mat Hashim, D., Mohamed, A.K.S., "Rapid identification of pork for halal authentication using the electronic nose and gas chromatography mass spectrometer with headspace analyzer", Meat Science, Vol. 88, No. 4, pp. 638-644, 2011.

[11] Song, S., Yuan, L., Zhang, X., Hayat, K., "Rapid measuring and modelling flavour quality changes of oxidised chicken fat by electronic nose profiles through the partial least squares regression analysis", Food Chemistry, Vol. 141, No. 4, pp. 4278-4288, 2013.

[12] Khot, L.R., Panigrahi, S., Doetkott, C., Chang, Y., "Evaluation of technique to overcome small dataset problems during neural-network based contamination classification of packaged beef using integrated olfactory sensor system", LWT - Food Science and Technology, Vol. 45, No. 2, pp. 233-240, 2012.

[13] D. Wang, X. Wang, T. Liu, Y. Liu, "Prediction of total viable counts on chilled pork using an electronic nose combined with support vector machine", Meat Science, Vol. 90, pp. 373–377, 2012

[14] Papadopoulou O., Panagou E.Z., Mohareb F., Nychas G-J., "Sensory and microbiological quality assessment of beef fillets, using a portable electronic nose in tandem with support vector machine analysis", Food Research International, Vol. 50, pp. 241–249, 2013

[15] Skandamis P., Nychas G.J., "Preservation of fresh meat with active and modified atmosphere packaging conditions", Int. Journal of Food Microbiology, Vol. 79, pp35– 45, 2002.

[16] , R. Paolesse, T. Boschi, M. Faccio, and G. Ferri, “An Electronic Nose for Food Analysis”, Sensors and Actuators B, Vol. 44, pp. 521-526, 1997
[17] V.S. Kodogiannis, M. Amina, I. Petrounias, “A clustering-based fuzzy-wavelet neural network model for short-term load forecasting”, Int. Journal of Neural Systems, Vol 23, No. 5, 2013.
[18] P. Jahankhani, V.S. Kodogiannis, J.N. Lygouras, I.P. Petrounias, “A Decision Support System for EEG signals based on Adaptive Inference Neural Networks”, Journal of Computational Methods in Sciences and Engineering (JCMSE), Vol. 11, No. 4, pp. 209-225, 2011
[19] Hubert M., Ousseeuw P., Branden K., “ROBPCA: A New Approach to Robust Principal Component Analysis”, Technometrics, Vol. 47, No. 1, pp. 64-79, 2005
[20] V.S. Kodogiannis, T. Pachidis, E. Kontogianni, “An intelligent based decision support system for the detection of meat spoilage”, Engineering Applications of Artificial Intelligence, Vol. 34, pp. 23–36, 2014.